Wear 526–527 (2023) 204925

Contents lists available at ScienceDirect

Wear

journal homepage: www.elsevier.com/locate/wear

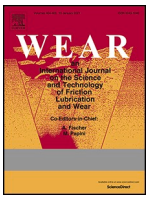

High-stress abrasive wear performance of medium-carbon direct-quenched and partitioned, carbide-free bainitic, and martensitic steels

Oskari Haiko [a,*], Sakari Pallaspuro [a], Vahid Javaheri [a], Pentti Kaikkonen [a], Sumit Ghosh [a], Kati Valtonen [b], Antti Kaijalainen [a], Jukka Kömi [a]

[a] Materials and Mechanical Engineering, Centre for Advanced Steels Research, University of Oulu, FI-90014, Oulu, Finland
[b] Materials Science and Environmental Engineering, Tampere Wear Center, Tampere University, FI-33720, Tampere, Finland

ARTICLE INFO

Keywords:
Steel
Microstructure
Abrasion
Wear testing

ABSTRACT

Experimental steels, a direct-quenched and partitioned (DQP) steel and a carbide-free bainitic steel (CFB), were tested along with a commercial martensitic 500 HB grade wear resistant steel in high-stress abrasive conditions. The three steels had different microstructures consisting of varying fractions and morphologies of martensite, retained austenite, and bainitic ferrite. The results showed that the CFB steel had a lower mass loss compared to the martensitic 500 HB steel with a similar hardness level. The DQP steel had a higher initial hardness and outperformed the other two steels. Wear surface characterization revealed that the investigated steels had significant work hardening of the wear surface, except with different mechanisms. Transformation induced plasticity (TRIP) increased the hardness of the DQP and CFB steels, while the fully martensitic 500 HB had more white layer formation on the wear surface resulting in increased hardness.

1. Introduction

Wear resistant steels are widely utilized in different applications in abrasive wear conditions. Most commercial wear resistant steels consist of a single-phase martensitic microstructure. However, steels with multiphase microstructures have become an increasingly interesting option as wear resistant materials. Recent studies have focused on two different steel variants in which retained austenite has a major role: the quenched and partitioned (Q&P) [1–3] and carbide-free bainitic (CFB) steels [4–7]. The former combines martensite with retained austenite to improve the toughness and ductility of the high-strength martensite. The main idea of Q&P processing is to enable the stabilization of the desired fraction of untransformed austenite at room temperature, which is achieved by interrupted quenching between the martensite start and finish temperatures, then followed by the partitioning at a desired temperature for a suitable period [8,9]. During the partitioning step, carbon is diffused out from supersaturated martensite into the untransformed austenite, which leads to stabilization of austenite at room temperature. Several compositions and processing routes have been studied to find the optimal combination of mechanical properties. On the other hand, direct quenching and partitioning (DQP) process is a modified approach to produce Q&P steels by removing the reheating stage and involving thermomechanical processing for refining the microstructure [10–13].

The DQP steels consist mainly of finely divided interlath retained austenite between the martensite blocks together with fractions of transition and/or cementite precipitates within tempered martensite, while the CFB steels might comprise several phases or microconstituents (i.e., bainitic ferrite, finely divided retained austenite within bainite blocks/plates together with fraction of primary/secondary martensite). The strength of CFB steels is derived from the extremely fine bainitic laths while the retained austenite provides ductility and toughness [14]. The transformation induced plasticity (TRIP) effect of the retained austenite is essential for both Q&P and CFB steels in enhancing the mechanical properties. Moreover, the retained austenite affects the work hardening of steel, and is thought to improve the wear resistance. In addition, the retained austenite has been reported to have an effect on crack initiation and propagation in a favorable manner [15,16]. If the energy of the particles inflicting wear is sufficient to transform the retained austenite into martensite, the wear surface hardness should increase and reduce wear. However, several factors affect the stability of retained austenite and the subsequent ability to transform into martensite [15,17,18].

The CFB steels have shown promising results in terms of wear

* Corresponding author.
E-mail address: oskari.haiko@oulu.fi (O. Haiko).

https://doi.org/10.1016/j.wear.2023.204925
Received 29 December 2022; Received in revised form 5 April 2023; Accepted 10 April 2023
Available online 12 April 2023

resistance. A great deal of research work has shown that the CFB steels may outperform some other steels in different wear conditions [5,19–21], even when tested against initially higher hardness steels [6]. The Q&P steels, on the other hand, have shown somewhat mixed results. In some studies, the Q&P steels have not shown better performance compared to fully martensitic counterparts [12], while there are also studies with improved wear resistance over some reference materials [2,3]. Additionally, it should be noted that the more traditional single-phase martensitic steels are still widely used as wear resistant materials and the research work for martensitic steels continues. Despite the differences in wear performance between steels with distinct microstructures, there are also great differences between the commercial martensitic steels in terms of wear resistance [22]. Some factors such as prior austenite grain size [23,24], tempering [25], and chemical composition [26] may have a drastic effect on the wear performance of martensitic steels. Furthermore, it appears that the martensitic steels also work harden to a great extent in harsh wear conditions [27] possibly improving the wear resistance. The current study was initiated to provide insight on the wear characteristics of novel CFB and DQP steels, and to compare these steels with a commercial martensitic steel. The research work was done to evaluate which of the steels would provide the best wear performance in the high-stress abrasive conditions.

In one of the authors' earlier studies, an experimental 0.3C DQP steel showed no clear improvement of wear resistance over a similar hardness martensitic steel in impact-abrasive conditions [12]. However, the latest iterations of the 0.4C DQP steel were studied for the microstructural features and mechanical properties in a recent study [28] showing promising results, and therefore one of these DQP steels was selected for wear testing. The new DQP steel has higher carbon and silicon contents, more retained austenite, and more austenite in the form of M/A islands compared to the previous version [12]. Likewise, the CFB steels tested in another study showed highly promising results for the wear performance [6], and hence one of these experimental steels was selected to be compared with the DQP steel. The selected CFB steel showed the best wear performance of the tested sixteen steels. For the comparison, a commercial 500 HB wear resistant steel was selected as a reference material. Therefore, the aim of this study was to compare the wear performance of these three steels with distinct microstructures to understand how the different microstructural features of the steels affect the high-stress abrasive wear performance. Comprehensive characterization of the wear surfaces was performed after wear testing, and work hardening has been discussed to clarify the differences in wear behavior between the three investigated steels and their respective microstructures.

2. Materials and methods

2.1. Processing and chemical compositions

Three steels were investigated in the study: two experimental steels (DQP and CFB) and one commercial wear resistant steel (500 HB). The chemical compositions of the steels are given in Table 1. Vacuum-casts for both the experimental steels were originally provided by OCAS NV, Belgium. The DQP cast was cut to smaller blocks with dimensions of 120 mm × 80 mm × 60 mm, which were soaked at 1200 °C for 2 h prior to two-stage laboratory hot rolling to a final thickness of 11 mm. The final rolling temperature was 820 °C, which was followed by direct quenching to a quench stop temperature of 150 °C. This was immediately followed by the partitioning treatment in a large-mass furnace set to 200 °C. The furnace was then switched off, and the plates were allowed to cool slowly for 24 h in order to simulate the cooling of coiled strips in the industrial hot rolling process. The plate temperature was around 80 °C after the 24 h cooling. A more detailed description of the DQP processing can be found in a previous study [28], where referred to as DQP-FC (Med-Si).

Table 1
Chemical compositions of the investigated steels (in wt.%, balance Fe). 500 HB showing the nominal maximum content.

Material	C	Si	Mn	Al	Cr	Mo	V	Nb
DQP	0.4	0.7	2.0	0.02	1.0	–	–	–
CFB	0.5	1.3	2.0	<0.01	0.7	<0.01	0.1	0.02
500 HB	0.3	0.8	1.7	–	1.5	0.5	–	–

The CFB ingots (150 mm × 150 mm × 500 mm) were homogenized at 1250 °C for 24 h followed by rough rolling to a thickness of 45 mm. After the annealing, 2 mm was milled away from both the upper and lower surface of the blocks, which were then cut to smaller dimensions for hot rolling. The reheating of the smaller blocks was done at 1250 °C for 90 min. Hot rolling was done above recrystallization temperature followed by cooling (20 °C/s) to 550 °C for two ausforming passes to reach the final thickness of 12 mm. Followed by the ausforming, the bainite transformation was ensured by isothermal holding at 350 °C for 90 min. The detailed processing route and previous wear test results of the CFB steel can be found in Ref. [6], abbreviated there as MT-E and more detailed information about the selection of the isothermal holding time in Ref. [29]. The commercial 500 HB wear resistant steel plate was selected as reference material for the wear testing. The same steel grade was used as reference material in the previous study [6].

2.2. Mechanical testing and microstructural characterization

Mechanical testing has been performed for the CFB and DQP steels in the two aforementioned studies [6,28], which included tensile and hardness (Vickers method) testing. A minimum of three tensile test samples or five indentations for hardness testing per experimental alloy were done. Wear surface hardness measurements were done with the Vickers HV0.05 method on tapered samples [6,22]: pieces were cut from the wear samples and cold-mounted at 10° angle to horizontal by using a taper section sample holder. The mounted samples were then ground, polished, and etched with Nital for hardness testing and microstructural characterization. The wear surface hardness was measured directly from the highly deformed surface as close as possible to the granite covered surface layer. At least three different spots were measured with each containing five indentations.

Initial microstructures and wear surfaces were characterized using Keyence VK-X200 laser scanning confocal microscope (LSCM) and Zeiss Sigma field-emission scanning electron microscope (FESEM). Samples were prepared by grinding, polishing, and Nital etching to reveal the microstructures. Phase volume fractions for the CFB steels were calculated by the point counting method according to ASTM E 562 standard [30]. Electron backscatter diffraction (EBSD, EDAX Hikari XP) and backscatter electron (BSE, Zeiss Sigma) were utilized to extract more information of the wear surfaces. The BSE imaging was utilized for the calculation of the fraction of area covered by granite with the aid of a Fiji image processing tool package based on ImageJ open-source image analysis software. Three images and analysis were done on each sample. Rikagu SmartLab 9 kW X-ray diffractometer (XRD) was used for determining the retained austenite content of the samples for both unworn and worn states. The measurements were done using a CoK_α source at a scanning rate of 7° min^{-1} over the range of 2θ = 24–130°. The diffraction peaks were analyzed by Rietveld refinement [31–33] and the phase fractions were calculated using PDXL2 software.

2.3. High-stress abrasive wear testing

Wear testing was performed at Tampere Wear Center, Tampere University, Finland, utilizing a pin-mill type dry-pot tester. The application-oriented high-stress abrasive testing device and similar parameters were also used for testing the CFB steel as in the previous study [6]. The device consists of a steel pot inside which a shaft fitted with

paddle-like samples is rotated in a gravel bed. Natural crushed granite from Kuru quarry, Finland, was used as the abrasive medium in the testing. The gravel was sieved to 8–10 mm size distribution and every batch of gravel weighed 9000 g. Fine quartzite (100–600 μm, Nilsiä quarry, Finland) was placed under the granite batch for every test period to ensure that the gravel would not pack underneath the shaft head. The shaft inside the pot was rotated at 250 rpm for a total of 240 min divided into 60-min test periods. For every 60-min test period, the samples were weighed, and the gravel was changed to a new fresh batch of sharp granite particles. Also, the sample position in the sample holder was changed for every period to ensure similar conditions for all samples during the 240-min test round. The sample size was 64 mm × 40 mm × 10 mm and the samples were fitted to the sample holder shaft at +45° angle to normal (Fig. 1). Four samples were tested at a time and two 240-min tests were conducted, which both consisted of one DQP, one CFB and two reference material samples. Thus, two samples were tested for the experimental materials (DQP and CFB) and four samples were tested for the commercial 500 HB material.

3. Results

3.1. Microstructure and mechanical properties

FESEM micrographs of the studied steels are shown in Fig. 2. The images show the bulk microstructure of each steel taken from 2.5 mm below the surface. As it has been previously presented [28], the DQP microstructure consisted of some fresh, but mostly tempered martensite with packets and blocks (Fig. 2a) inside the parent austenite grains. Needle-like transition carbides could be seen, and the number of carbides was extensive indicating that the martensite was strongly tempered during the long (24 h) partitioning process. In addition to the martensitic matrix, some martensite/austenite (M/A) islands were present shown in Fig. 2a'. Transmission electron analysis [28] had shown that DQP steel exhibited also finely dispersed interlath retained austenite present not visible in the FESEM micrographs. The analysis of the DQP steels revealed that the grain structure was slightly elongated owing to the hot rolling below the recrystallization temperature. The prior austenite grain size was estimated to be around 20 μm (mean linear intercept method [34]). The retained austenite content for the DQP steel was 13% (XRD).

The CFB steel showed different microconstituents in the microstructure: bainitic ferrite, some martensite, and M/A islands (Fig. 2b and b'). The steel had a multiphase structure with estimated phase average fractions of 61% of bainitic ferrite (BF), 16% of martensite (grid point counting method), and 22.9% of retained austenite (RA) (XRD) [6]. The CFB microstructure appeared more heterogeneous compared to the martensitic steels showing some local differences in the fraction of different microconstituents. Martensite was in the form of martensite/austenite (M/A) islands. The bainitic ferrite features, which included all bainitic features (laths, plates, granular bainite), was measured with image analysis, and resulted in average size of 368 ± 24 nm [6]. The average size was somewhat larger than often reported for CFB steels [35, 36].

The 500 HB steel (Fig. 2c and c') had a typical lath-type martensitic microstructure with number of small transition carbides in the structure, presumably formed due to autotempering. The commercial 500 HB steel showed no retained austenite (<1%, below detection accuracy) present in the microstructure (XRD). Both martensitic DQP and 500 HB steels had quite similar microstructures with tempered martensite (TM) and transition carbides as the main constituents, while the major differences were the retained austenite content DQP: 13%, 500 HB: <1%) and the amount of fresh martensite (FM) (visibly higher for 500 HB).

The mechanical properties of the steels are presented in Table 2. Tensile properties for the 500 HB steel are typical values from the product sheet provided by the manufacturer. The DQP steel had the highest strength and hardness, while the CFB had slightly better uniform elongation possibly due to the higher retained austenite content or different morphology of the austenite. Compared to the commercial 500 HB steel, the two experimental steels had very low yield-to-tensile strength ratio owing to the retained austenite and subsequent TRIP effect and work hardening. However, it should be noted that these types of steels rarely exhibit sharp yield limit, thus the 0.2% offset yield strength is given. Both the yield strength and tensile strength were higher for the DQP compared to the CFB. Furthermore, the initial bulk hardness was higher for the DQP (594 HV) while the CFB and 500 HB steels had similar hardness of 535 HV.

3.2. Wear test results

The measured mass loss from the dry-pot testing is given in Table 3 along with values for the initial hardness, wear surface hardness, and retained austenite content measured prior to and after the wear testing. The DQP steel had the lowest mass loss (1.310 ± 0.011 g) followed by the CFB (1.371 ± 0.028 g) and 500 HB (1.417 ± 0.014 g). The mass loss and initial hardness/wear surface hardness did not show linear correlation.

The wear surface hardness measured from the tapered samples revealed large increase for the hardness. The DQP had the highest wear surface hardness (896 HV0.05), but the highest relative increase in hardness was measured for the 500 HB steel (+60%). The deviation for

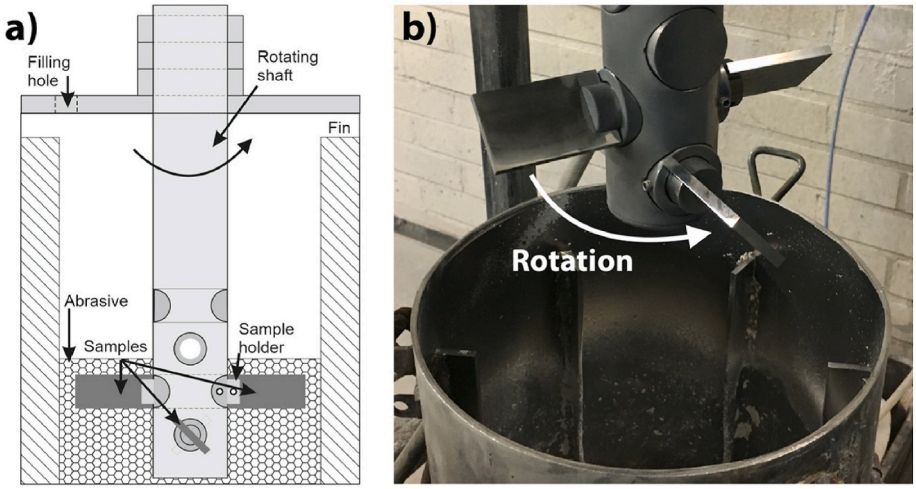

Fig. 1. a) Schematic illustration of the high-stress abrasive tester (dry-pot) and b) image of the tester fitted with four samples at +45° angle [23].

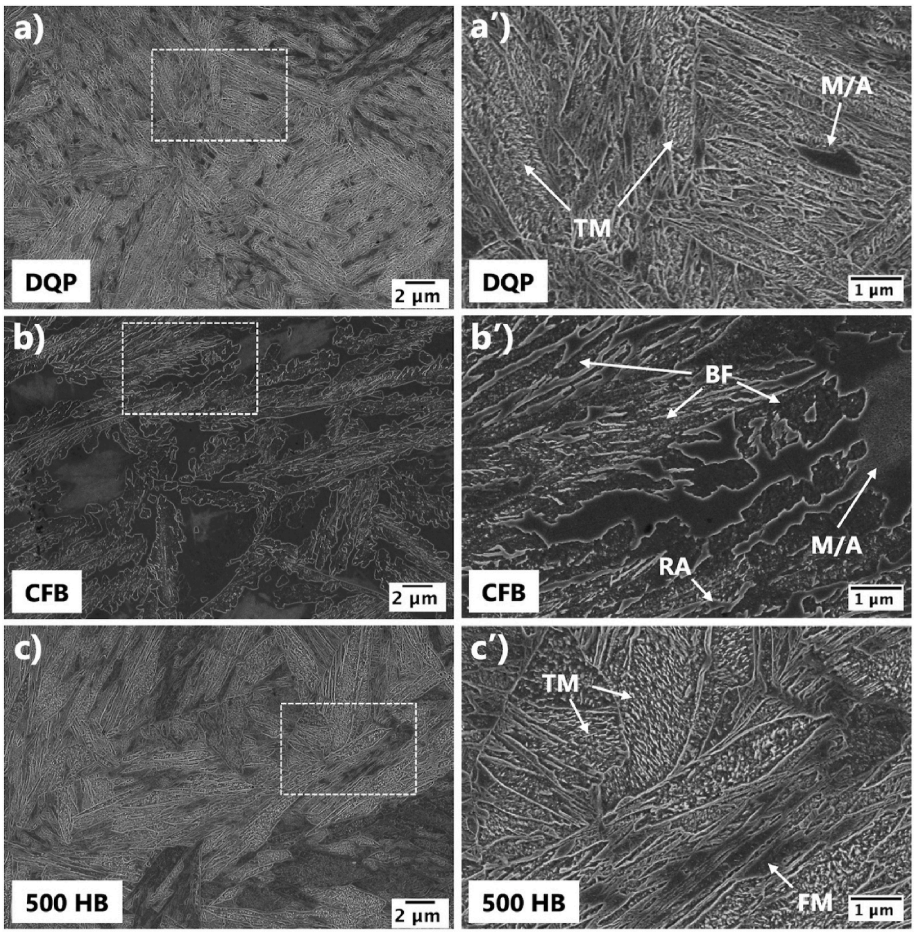

Fig. 2. Typical bulk FESEM micrographs of the investigated a-a') DQP, b-b') CFB, and c-c') 500 HB steels with close-up images on the right (TM: tempered martensite, M/A: martensite/austenite, RA: retained austenite, BF: bainitic ferrite, FM: fresh martensite).

Table 2
The mechanical properties (0.2% offset yield strength ($R_{p0.2}$), ultimate tensile strength (R_m), yield-to-tensile strength ratio, uniform elongation (A_g) and bulk hardness (HV10) and retained austenite volume content of the investigated steels. 500 HB yield and tensile strength as received in from product data sheet.

Material	$R_{p0.2}$ [MPa]	R_m [MPa]	Yield ratio	A_g [%]	Hardness [kgf/mm^2]	Retained austenite [%]
DQP [28]	918 ± 36	2086 ± 44	0.44	7.1 ± 0.2	594 ± 8	13 ± 1
CFB [6]	821 ± 10	1912 ± 9	0.43	7.9 ± 0.6	535 ± 22	22.9 ± 1
500 HB	1300	1600	–	–	535 ± 16	<1

the wear surface hardness was large due to the highly localized surface deformation.

Retained austenite measured directly from the wear surface showed that for the DQP all austenite had transformed during the high-stress abrasive testing. The CFB with higher initial retained austenite content had some retained austenite (6.2%) still present after the wear testing. The retained austenite volume fractions of 500 HB were below the determination limit both prior and after the wear testing.

3.3. Wear surface characterization

The wear surfaces of the investigated steel samples were characterized from the side (LSCM, FESEM, EBSD) and from above (LSCM: tapered samples, BSE). The cross-sectional view of the wear surfaces is shown in Fig. 3. The panorama images were taken with the LSCM by stitching several images together using the combination of laser images for sharpness and optical images for the colors. Granite particles had

Table 3
Wear test results with hardness and retained austenite values.

Material	Mass loss [g]	Bulk hardness HV10 [kgf/mm^2]	Wear surface hardness HV0.05 [kgf/mm^2]	Hardness increase	Retained austenite – prior [%]	Retained austenite – after [%]
DQP	1.310 ± 0.011	594 ± 8	896 ± 87	+51%	13 ± 1	<1
CFB	1.371 ± 0.028	535 ± 22	834 ± 62	+56%	22.9 ± 1	6.2 ± 0.5
500 HB	1.417 ± 0.014	535 ± 16	856 ± 51	+60%	<1	<1

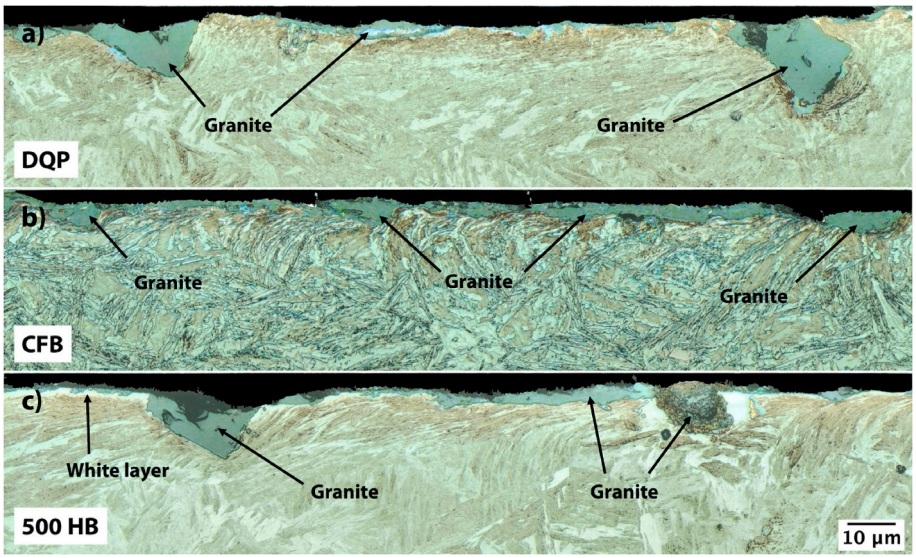

Fig. 3. Laser-optical panorama images of the wear surface cross-sections of the three investigated steels: a) DQP, b) CFB, and c) 500 HB. Abrasive flow from left to right.

embedded in all the samples, which is typical for steel samples tested with a dry-pot method. Also, a shallow tribolayer with a mixture of steel and granite had formed on all samples.

Starting with the DQP, the wear test sample had some visible deformation in the wear surface, however the depth of deformation was somewhat difficult to estimate. A closer investigation revealed that some deformed structures could be seen reaching a depth of approximately 15 μm from the surface. A mixture of steel and granite had formed a tribolayer on the surface, however no substantial amount of white etching layer [27,37] was detected. The CFB, on the other hand, also showed plastically deformed structures near the wear surface and some parts of the deformed microstructure appeared to have more white areas or features. This cannot be clearly stated to be the white layer, but it could be a martensitic layer formed due to the TRIP effect, which was expected based on the amount of retained austenite present (22.9%). It has been previously discussed that the CFB steels might not be as susceptible as martensitic steels to form white layer in abrasive conditions [6]. Opposing the observations for the other two steels, the fully martensitic 500 HB steel had some clearly visible white layer formed on the wear surface. It was noted that the microstructure was deformed and elongated in the direction of the abrasive flow, which is often seen with such martensitic steels [22,23]. The depth of deformation did not differ drastically from the other steels; generally, around 10–15 μm.

Montage images were also created from the tapered samples to show the top view of the wear surfaces in Fig. 4. The grey, greenish area on the top of the images is the granite covered surface layer. Due to the tapered sections, the scale bar (40 μm) is valid only for the horizontal direction. Vertical movement for the length of the scale bar corresponds to approximately 7 μm in depth revealing the deformed microstructure just underneath the granite covered tribolayer. The white layer can be seen better in these images for the DQP (Fig. 4a) and 500 HB (Fig. 4c). Some small areas of the white layer were visible in the wear surface of the DQP, whereas white areas were drastically thicker for the 500 HB steel. The CFB steel did not show any or only very minor areas of the white layer. Therefore, it could be speculated that the increase in hardness was caused by different microstructural features for the CFB steel; the transformation of austenite to martensite (TRIP) and work hardening of the bainite and martensite. These images also showed how the granite had penetrated the surface and mixed with the deformed steel. In this matter, the CFB appeared to have the thickest layer of this mixed tribolayer of steel and granite, whereas the interface of the granite covered surface and bulk microstructure was sharper for the 500 HB, and for the DQP it was somewhere in between.

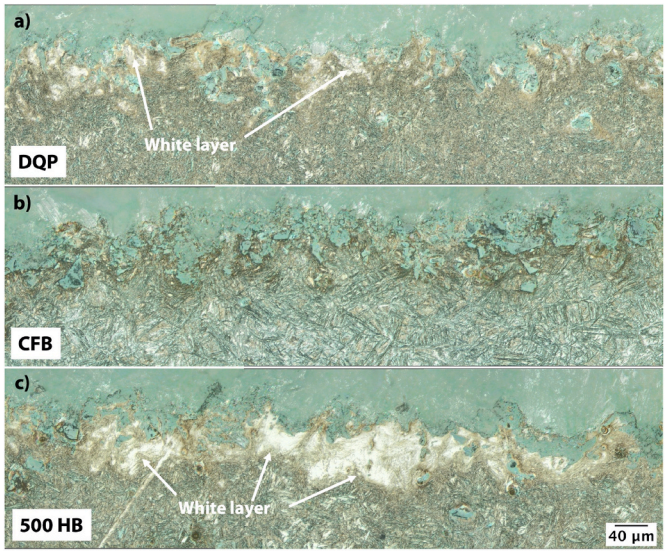

Fig. 4. Laser-optical montage images of the tapered samples: a) DQP, b) CFB, and c) 500 HB.

FESEM images of wear surface cross-sections of the investigated steels are shown in Fig. 5. The microstructures have been heavily deformed for all the samples, but the depth of deformation was quite low as already seen with the laser-optical images. Naturally, some material has been removed from the surface, but in general, the abrasion has inflicted damage very close to the surface. The elongated structures are the most distinct features caused by the abrasion. However, the severity of the deformation changes throughout the deformed structures: two distinct regions are visible in the close-up images (Fig. 5), especially for the DQP (Fig. 5a) and CFB (Fig. 5b) steels. The DQP shows some areas (marked with I in Fig. 5a) with quite undistinguishable microstructure i.e., very fine-scale constituents are presumably present. On the other hand, the CFB steel also shows two different regions of deformed microstructure, but the area (II in Fig. 5b) appears different from the severely deformed region of the DQP steel. In contrast to the other two steels, the 500 HB (Fig. 5c) did not show such severely deformed regions to the same extent, while the deformation was more in the form of

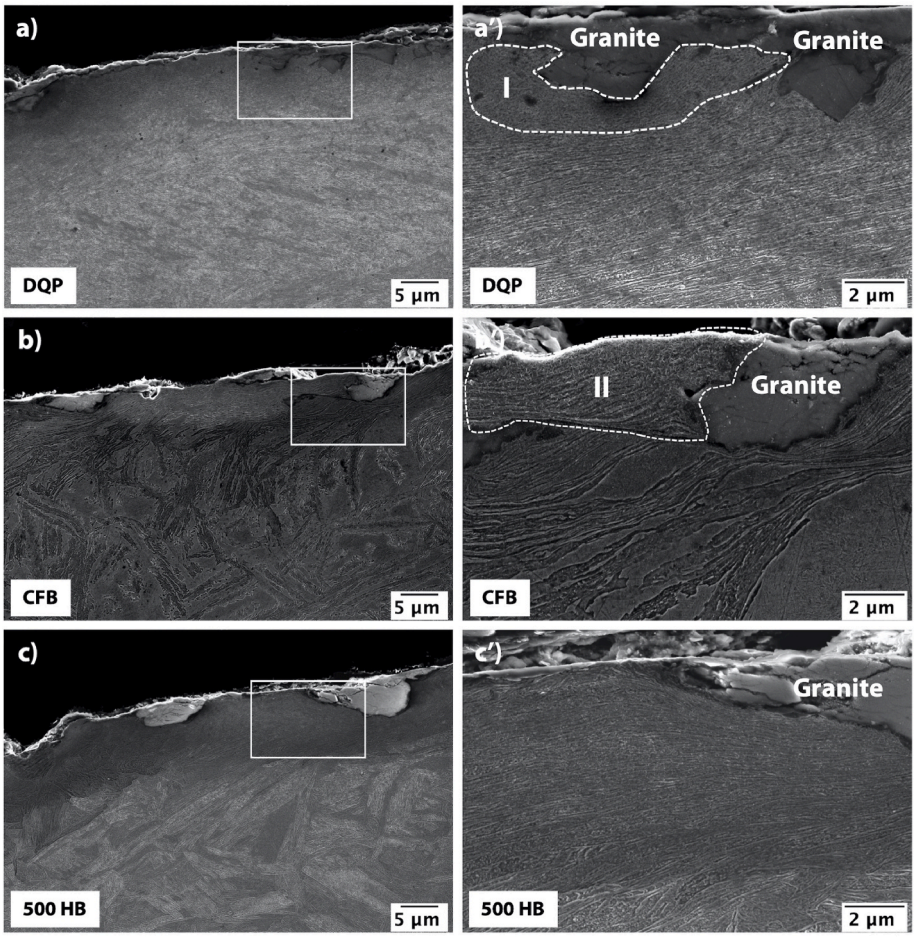

Fig. 5. FESEM cross-sectional images of the wear surfaces with close-up images on the right: a-a') DQP, b-b') CFB, and c-c') 500 HB.

elongated constituents presumed to be the highly deformed martensitic sub-structure (laths, packets).

The BSE images, in Fig. 6, were taken directly on the granite covered surface. The amount of granite (dark areas) embedded in the wear surfaces was substantial. The close-up images in Fig. 6 show the typical abrasion marks of microploughing and microcutting, which are often found after high-stress abrasive testing. Some possible lip formation was found, but no clear evidence of delamination could be confirmed. The plastic deformation was visible in the form of multiple grooves and furrows caused by the abrasives. It can be expected that the ploughed material on the groove ridges is eventually removed by the constant plastic deformation caused by the granite particles, either by cutting or fatigue. The BSE imaged surfaces were quite similar between the steel samples, though the CFB steel showed more of small pits on the surface. Also, the fraction of granite covered surface area was estimated higher for the 500 HB steel compared to the other two steels. The surface area covered in granite was calculated from BSE images and averaged 59 ± 3% for the DQP, 57 ± 4% for the CFB, and 62 ± 3% for the 500 HB.

Fig. 7 presents the inverse pole figure (IPF) and image quality (IQ) EBSD maps of the wear surface cross-sections for all the investigated specimens. In the case of the DQP sample with the martensite as the matrix and reference material (500 HB) with a fully martensitic microstructure, a severely deformed surface layer along the wear direction is clearly observed. The severe deformation and straining of martensite produced a very fine structure and high hardness level in this surface layer. As listed in Table 3, these two samples achieved higher final hardness after the wear testing compared to the CFB sample. Likewise, in the previous study [27], it has been demonstrated that martensite could accommodate multidirectional impacts and severe plastic deformation by creation, movement, and rearrangement of dislocations. This could result in formation of nanocrystalline and sub-structure (in the range of few hundred nanometers) surface layer having low- and high-angle grain boundaries and extremely high hardness value. However, in the case of DQP, the deformation can initially be accommodated by the deformation of retained austenite and the subsequent transformation of retained austenite to fresh martensite. Both the XRD and the EBSD investigations of the wear area of the DQP sample indicated that almost all retained austenite transformed to martensite during abrasive wear. Both the formation of nanocrystalline structure due to the deformation of old martensite matrix as well as the formation of nano-scaled fresh martensite as a result of stress induced transformation of retained austenite increase the hardness of the surface layer and furthermore can be assumed to improve the wear resistance [5].

In the case of the CFB sample, the deformed surface has a slightly coarser structure than those of the two other owing to the ductile bainitic matrix which can accommodate more deformation than martensite as well as the higher fraction and higher stability of retained austenite. In agreement with the XRD results, as given in Fig. 8, the EBSD characterization similarly revealed that there was still some retained austenite remaining on the wear surface and sub-surface. This indicates higher mechanical stability of retained austenite in the CFB sample compared to the DQP steel; presumably due to the higher carbon content of the CFB steel. Based on the data presented in Fig. 8b, it appeared that the large and blocky type of retained austenite with specific crystal orientations had exhibited remarkable stability during the severe straining of the wear test. However, in order to obtain a more comprehensive understanding of this phenomenon, further investigations utilizing additional techniques such as high-resolution electron backscatter

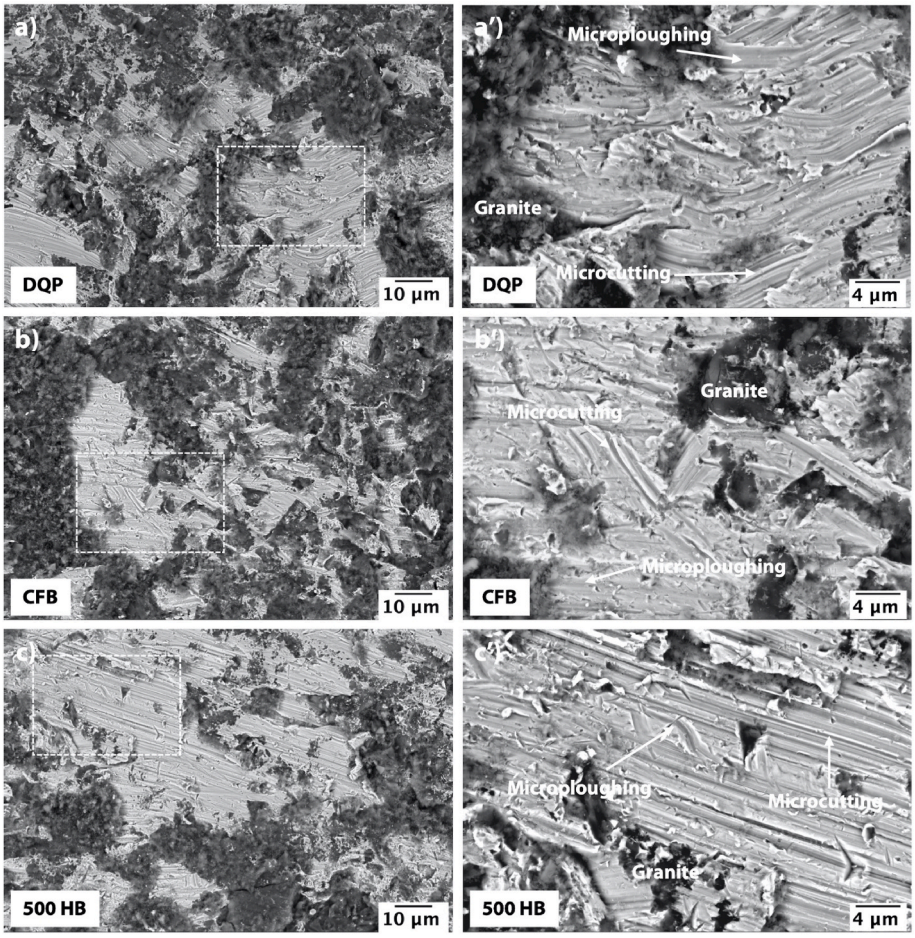

Fig. 6. BSE images of the wear surfaces with close-up images on the right: a-a') DQP, b-b') CFB, and c-c') 500 HB.

diffraction (HR-EBSD) and transmission electron microscopy (TEM) are necessary. These techniques will allow for a more detailed analysis of the orientation relationship between retained austenite, initial martensite, and mechanically-induced martensite and provide additional insights into their behavior during the wear test.

4. Discussion

The two experimental steels (DQP and CFB) showed very good wear performance when tested in high-stress abrasive conditions. Both steels outperformed the martensitic 500 HB wear resistant steel, though the initial hardness for the DQP steel was higher. Regarding the mechanical properties, the most interesting feature for the DQP and CFB was the low yield-to-tensile strength ratio (<0.5): the yield strength was less than 1000 MPa for both steels, however the tensile strength reached up to 2000 MPa indicating very high strain-hardening during the tensile testing. Though it cannot be stated clearly that the tensile properties would have a connection on the wear performance, the yield ratio did indicate that substantial work hardening would be expected later to be confirmed by the hardness increase of the wear surfaces. Another distinct feature of the mechanical properties of the DQP and CFB steels was the bulk hardness: both steels had high initial hardness (>500 HV) compared to the yield strength (800–900 MPa), another character of high work hardening ability. Although, it should be borne in mind that the determination of 0.2% offset yield strength is somewhat ambiguous for such steels with no sharp yield limit. Nevertheless, the key finding here was that connecting the quasi-static mechanical properties of a given steel and abrasive wear resistance is quite difficult [38], and mechanical properties can only be treated as one of many implications for the wear resistance in abrasive conditions.

The high-stress abrasive wear testing method produced severe wear on all the investigated steels. Heavy abrasion was the main wear mechanism inflicted by the crushed granite particles. The BSE images of the wear surfaces (Fig. 6) showed that microploughing and microcutting resulted in the main damage, but it can be assumed that some of the ploughed material was eventually removed by surface fatigue. Granite particles had been embedded in the wear test samples and the fraction of granite covered area was substantial for all the samples. It has been debated whether the abrasive particle embedment could provide some protection against wear in crushing pin-on-disc testing [39,40], but such phenomenon has not been discovered in dry-pot testing [25]. In the current study, the CFB had the lowest fraction of granite coverage, but it did not show the lowest mass loss. On the other hand, the 500 HB had the highest mass loss and the highest fraction of granite covered surface area. Therefore, it was concluded that the granite embedment did not provide any additional protection against the abrasive wear in the current test conditions.

The steels were prone to severe deformation leading to accumulation of strain and subsequent work hardening. The microstructures of the investigated steels comprised different phases and microconstituents resulting in different wear behavior. Initially, the steels exhibited hardness greater than 500 HV, but substantial work hardening occurred during the wear testing. The deformed wear surfaces had hardness in the range of 800–900 HV, while bulk hardness was less than 600 HV for all three steels. The DQP had the highest wear surface hardness, but the difference was not that prominent: the difference in the initial hardness was actually lower compared to the difference in wear surface hardness. The DQP had a 4.4% lower mass loss compared to the CFB and 7.6%

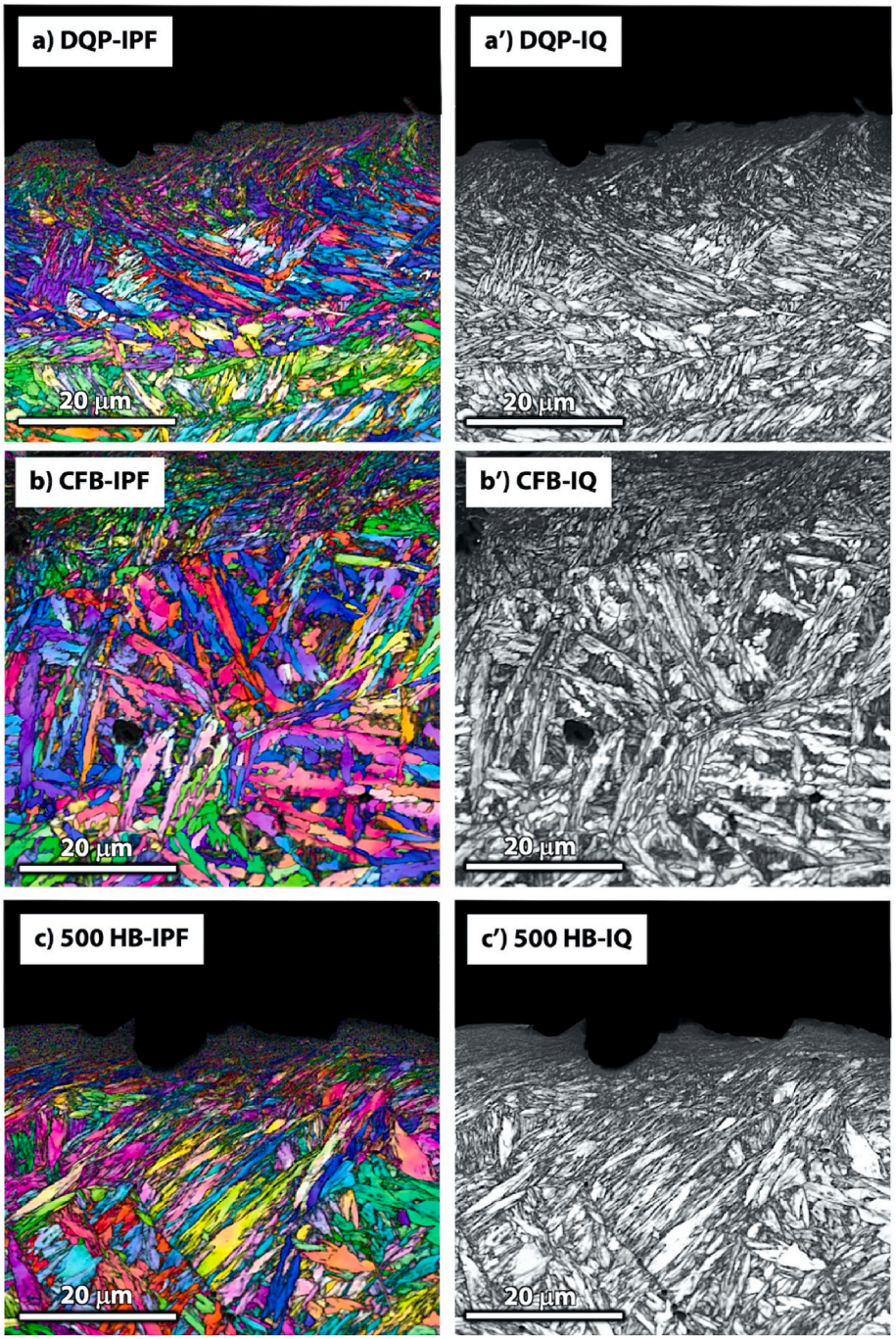

Fig. 7. Inverse pole figure (left) and image quality (right) EBSD maps of the wear surfaces of the investigated steels: a-a') DQP, b-b') CFB, and c-c') 500 HB.

lower compared to the 500 HB. The initial hardness was 11% higher for the DQP compared to CFB and 500 HB, whereas the wear surface hardness was 7.4% (CFB) and 4.7% (500 HB) higher for the DQP, respectively. Therefore, the correlation between either of the hardness values, initial or wear surface, with mass loss was not as straightforward as expected. In the two previous studies with DQP and CFB steels, either the initial hardness [12] or the wear surface hardness [6] correlated well with the wear performance, but in both studies the reference 500 HB steel was excluded from the linear correlation. Therefore, it can be still debated whether the correlation between either initial hardness or wear surface hardness and mass loss is only valid for the steels of similar microstructure or composition. However, the wear surface hardness was measured from the interface between the granite-covered surface and the deformed structure beneath from the tapered samples as close as possible to the surface. This method does not account for whether the indentation has been made on white layer, shear band, or deformed microstructure. As the white layer and shear bands tend to exhibit significantly higher hardness over the less severely deformed microstructure [22], the comparison of hardness favors those steels with more white layer formation. It can be debated whether the 500 HB had higher average wear surface hardness due to the presence of very hard white layer when compared to the CFB sample. The white layer formed during wear processes has been discussed whether it can improve or deteriorate wear resistance in steels [27,37,41]. The significant increase in wear surface hardness of the 500 HB was presumably caused by the extremely hard white layer, which in turn might have decreased the wear performance when compared to the CFB steel with lower hardness, but absence of white layer. The extremely fine and hard white layer resists

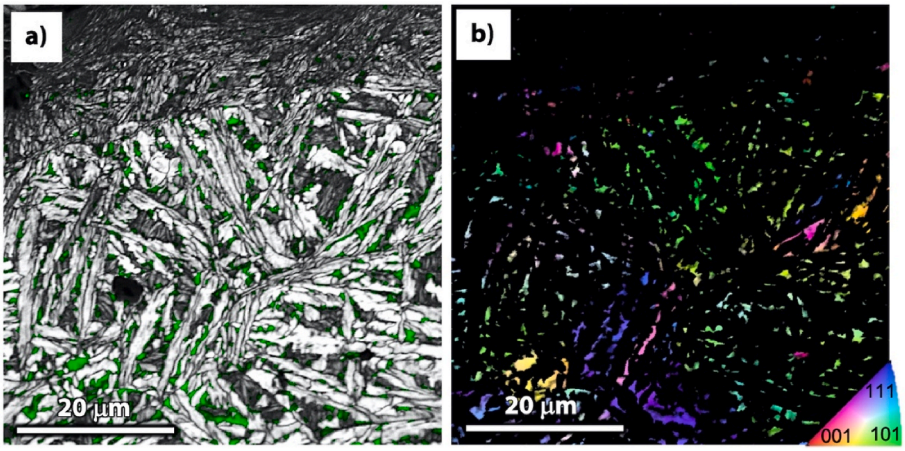

Fig. 8. Retained austenite distribution in the CFB sample wear surface: a) Image quality (austenite in green) and b) inverse pole figure map of retained austenite distribution of the CFB wear surface sample (EBSD). (For interpretation of the references to color in this figure legend, the reader is referred to the Web version of this article.)

microcutting, but the large hardness gradient between this layer and the bulk microstructure creates a possible pathway for cracks to propagate resulting delamination or spalling. Furthermore, the high-hardness white layer is more prone to surface fatigue due to the decreased capability to plastic deformation. However, the wear conditions leading to such behavior are more likely to occur when severe impact loading is present [27,41] whereas the current wear test conditions were more abrasive. On the other hand, the DQP steel did show some white layer and very fine features in the wear surface, but possibly the TRIP effect reduced possible deteriorating effect of the white layer on the wear performance. Also, the area covered by white layer was less for the DQP compared to the 500 HB.

The CFB and 500 HB steels were also tested in the previous study [6], where both were measured a slightly higher mass loss, which could have been caused by the use of a newer batch of granite provided by the quarry. However, the difference between the two also slightly varied. Here, the mass loss for the CFB steel was 3.2% lower compared to the 500 HB, whereas in the previous tests the difference in the mass loss was 5.8% in favor of the CFB. The CFB had similar wear surface hardness in both studies, but the 500 HB had around 50 HV higher wear surface hardness in this study. This indicates that the wear performance had slightly increased for the 500 HB steel. The change in the wear performance of the 500 HB might have been caused by some local deviation within the material or by a slightly different batch of material, which essentially led to higher work hardening and marginally better wear performance. Also, previously [6] the RA content for the CFB steel after wear testing was 3.9% while now it was measured 6.2%, which might partially explain differences in the wear performance when comparing to the 500 HB steel. The deviation for the testing method and tested materials (when cut from the same plate) are generally very low, less than 3%.

The most interesting feature of the study is how the steels showed high work hardening. Considering the different compositions, microstructures, and evidently different wear surfaces, it could be stated that all steels showed a great degree of work hardening, but this most likely occurred by slightly different mechanisms. It can be assumed that the TRIP effect played a major role in the work hardening of DQP and CFB steels. The amount of retained austenite had decreased significantly for both the DQP and the CFB indicating that strain-induced martensite had formed during the wear testing leading to higher hardness. All of the RA had diminished from the surface of the DQP steel, but the CFB still had 6.2% austenite present. Therefore, it can be stated that part of the work hardening for the two experimental steels is explained by the TRIP effect, while some part of work hardening is presumably caused by the deformation and work hardening of the surrounding matrix. Furthermore, the effect of retained austenite on the abrasive wear performance can be concluded positive for the investigated steels.

The DQP steel consisted of martensite and retained austenite, thus the work hardening of martensite was also expected. However, it is somewhat difficult to distinguish how much of the hardness increase each of the two different work hardening mechanisms accounted for. Moreover, as no retained austenite was detected on the wear surface of the DQP sample, it can be stated that the stability of the interlath RA was not too high for the TRIP effect to take place. The initial RA content was 13% and the carbon content of the RA was 0.59 wt%, whereas after the tensile testing the RA content was below 1% [28]. Despite the thermal stability of the film-like residual austenite in the DQP steel, which is stable at room temperature, it will readily transform to martensite under straining and also during the high-stress abrasive wear testing. Furthermore, the wear surface will have two different martensite present during wear: the initial martensite formed during quenching and the transformation induced martensite due to the TRIP. Both will be subjected to severe plastic deformation and subsequent work hardening. With current characterization methods, it is challenging to distinguish the role of these two martensitic phases in the wear resistant properties of the DQP steel in abrasive conditions. However, some TEM images have proven that mechanically induced twins have been discovered in the strain induced martensite along with very high dislocation density [2]. As for the CFB steels, it has been proposed that the severely deformed layer with final structure of equiaxed nano-sized grains is originated from both ferrite and austenite: the ferritic structure transforms into nanograins due to the dislocations while austenite would depend on twins and dislocations [42]. This confirms that the resulting strain induced martensitic structures have different properties to some extent.

The CFB steel had more phases present with different morphologies making the work hardening more complicated to study. The total amount of bainitic ferrite was estimated 61% including all bainitic ferritic features (bainitic laths and plates, granular bainite) making bainite the dominating phase in the initial microstructure compared to martensite (16%) and retained austenite (22.9%). As mentioned, the TRIP effect was presumed to influence the work hardening similar to the DQP steel regarding the role of retained austenite. As the wear surface of the CFB steel appeared somewhat different from the two martensitic steels, it can be speculated that TRIP and the following work hardening of the wear surface does differ from martensite (500 HB) or martensite with retained austenite (DQP) due to the presence of other phases. The bainitic matrix also resisted the abrasion and the deformed and elongated microstructure was seen in the FESEM images (Fig. 5b and b'). The EBSD results (Fig. 7b and b) also confirmed the gradual change from the

most worn part to the less severely deformed structure for the CFB. The topmost layer consisted of very fine structures of the highly deformed bainite, martensite, and transformed martensite with some retained austenite. Accordingly, the wear surfaces of the 500 HB and the DQP essentially transformed into fully martensitic structures during wear, while this did not occur with the CFB based on the EBSD and XRD measurements, and retained austenite was still present after wear testing (6.2%). The carbon content for the retained austenite in the CFB steel was estimated in an earlier study to be 1.01 wt% [43], which would explain higher stability of the RA during abrasive wear and the amount of untransformed RA in the wear surface. In addition, the laser-optical images of the CFB sample (Figs. 3b and 4b) showed the absence of white layer.

Likewise in the DQP sample, the main fraction of retained austenite in the CFB sample transformed into hard martensite during severe plastic deformation caused by particle impacts. This resulted in the hardening of the surface and sub-surface layers where the volume fraction of induced martensite decreased with sub-surface depth as the severity of plastic deformation decreased from surface towards the bulk. It has been reported that in CFB steels the formation of nanoscale martensitic laths from the retained austenite could reduce the void and crack formation beneath the wear surface by absorbing the energy from the repeated particle impacts and enhances the abrasive wear resistance [15,44]. The high-stress abrasive conditions in this study caused repetitive microploughing and microcutting; the retained austenite transformed into martensite during the ploughing (deformation) while the strain-induced martensite later resisted cutting. It can be also speculated that the different morphologies of the retained austenite in the CFB steel (blocky, film-like, M/A islands) [15] affect the TRIP effect and the resulting microstructure differently, which essentially then acts as the new wear surface. In high-stress wear conditions, the film-like interlath, more stable austenite has been proven to provide better wear resistance, i.e. the ratio between interlath and blocky austenite should favor the former type [7]. The same study also suggested that the martensite induced from the film-like austenite might provide structure less prone to crack formation compared to the martensite induced from the blocky austenite. In addition, the volume expansion due to the face-centered cubic to body-centered cubic transformation could act as crack closure mechanism [45]. Still, the stable austenite could have two-fold effect on the wear performance: crack-tip blunting and absorbing crack propagation energy might be useful [46], but the essentially lower hardness of the austenite might prove detrimental.

The freshly formed microstructure will have different interactions with the initial and newly formed microconstituents and this finally determines the wear resistance of the CFB steel in the wear conditions with continuous deformation of the wear surface. It should be borne in mind that deformation during wear will reach further underneath into the sub-surface: as the topmost layer eventually wears out the layers beneath have already been subjected to deformation and microstructural changes [47]. Hence, all the differently deformed layers will influence the wear resistance. As a summary, the deformation of different phases during abrasive wear creates a highly complex phenomenon, and the role of each phase, especially in worn and deformed state, could not be explained thoroughly here. Therefore, it is interesting that all steels eventually exhibit slightly different wear performance achieved by different mechanisms.

5. Summary and conclusions

The study encompasses the characterization of high-stress abrasive wear performance of three steels with distinct microstructures. A commercial 500 HB martensitic wear resistant steel was compared with experimental carbide-free bainitic (CFB) and direct-quenched and partitioned (DQP) steels. After wear testing and subsequent microstructural characterization, the following conclusions were made:

1. The DQP steel had the lowest mass loss in wear testing while the CFB steel outperformed the similar hardness level 500 HB martensitic steel. The DQP steel had the highest initial hardness and the highest wear surface hardness measured after wear testing.
2. Wear surfaces hardened to a high degree in all investigated steels, although with different mechanisms. The DQP and CFB steels had retained austenite transformed into martensite due to the TRIP resulting in increased wear surface hardness. The martensitic 500 HB steel had pronounced white layer formation along with grain refinement on the wear surface leading to increased surface hardness.
3. All investigated steels showed very fine deformed structures in the wear surfaces. Retained austenite transformed completely into martensite in the DQP steel while the CFB steel had still some austenite present in the immediate vicinity of the wear surface.
4. The dry-pot high stress abrasive testing inflicted wear damage mostly by microploughing and microcutting mechanisms. The granite particles had caused severe plastic deformation seen in the wear surfaces as ploughed material and grooves.

Author statement

Oskari Haiko: Writing - original draft, Formal analysis, Investigation, Resources, Visualization, Data curation, Conceptualization, Revision.

Sakari Pallaspuro: Writing - original draft, Investigation, Data curation, Funding, Revision.

Vahid Javaheri: Writing - original draft, Formal analysis, Data curation, Revision.

Pentti Kaikkonen: Writing - original draft, Formal analysis, Resources, Revision.

Sumit Ghosh: Writing - original draft, Resources, Revision.

Kati Valtonen: Writing - review & editing, Resources.

Antti Kaijalainen: Writing - review & editing, Supervision, Revision.

Jukka Kömi: Project administration, Supervision.

Declaration of competing interest

The authors declare that they have no known competing financial interests or personal relationships that could have appeared to influence the work reported in this paper.

Data availability

Data will be made available on request.

Acknowledgments

This research has been done within the Business Finland program Fossil Free Steels and Applications (FOSSA, Dno. 5397/31/2021) and the Academy of Finland project PerforMat (#337108 & 337941). We gratefully acknowledge the financial support and the companies participating in the FOSSA program. Part of the work was carried out with the support of the Centre for Material Analysis, University of Oulu, Finland.

References

[1] J. Lai, L. Zhang, W. Gong, X. Xu, C. Xiao, Two-body abrasion resistance of high carbon steel treated by quenching-partitioning-tempering process, Wear 440–441 (2019), 203096, https://doi.org/10.1016/j.wear.2019.203096.

[2] J. Lu, H. Yu, P. Kang, X. Duan, C. Song, Study of microstructure, mechanical properties and impact-abrasive wear behavior of medium-carbon steel treated by quenching and partitioning (Q&P) process, Wear 414–415 (2018) 21–30, https://doi.org/10.1016/j.wear.2018.07.026.

[3] C. Wang, X. Li, Y. Chang, S. Han, H. Dong, Comparison of three-body impact abrasive wear behaviors for quenching–partitioning–tempering and

quenching–tempering 20Si2Ni3 steels, Wear 362–363 (2016) 121–128, https://doi.org/10.1016/j.wear.2016.05.026.
[4] A.M. Gola, M. Ghadamgahi, S.W. Ooi, Microstructure evolution of carbide-free bainitic steels under abrasive wear conditions, Wear 376–377 (2017) 975–982, https://doi.org/10.1016/j.wear.2016.12.038.
[5] M. Shah, S. Das Bakshi, Three-body abrasive wear of carbide-free bainite, martensite and bainite-martensite structure of similar hardness, Wear 402–403 (2018) 207–215, https://doi.org/10.1016/j.wear.2018.02.020.
[6] O. Haiko, P. Kaikkonen, M. Somani, K. Valtonen, J. Kömi, Characteristics of carbide-free medium-carbon bainitic steels in high-stress abrasive wear conditions, Wear 456–457 (2020), 203386, https://doi.org/10.1016/j.wear.2020.203386.
[7] Z. Wei, W. Wang, M. Liu, J. Tian, G. Xu, Comparison of wear performance of bainitic and martensitic structure with similar fracture toughness and hardness at different wear conditions, Wear 512–513 (2023), 204512, https://doi.org/10.1016/j.wear.2022.204512.
[8] J. Speer, D.K. Matlock, B.C. De Cooman, J.G. Schroth, Carbon partitioning into austenite after martensite transformation, Acta Mater. 51 (2003) 2611–2622, https://doi.org/10.1016/S1359-6454(03)00059-4.
[9] J.G. Speer, F.C.R. Assunção, D.K. Matlock, D.V. Edmonds, The "quenching and partitioning" process: background and recent progress, Mater. Res. 8 (2005) 417–423, https://doi.org/10.1590/S1516-14392005000400010.
[10] M. Somani, D. Porter, L. Karjalainen, K. Devesh, Evaluation of DQ&P processing route for the development of ultra-high strength tough ductile steels, Int. J. Metall. Eng. 2 (2013) 154–160, https://doi.org/10.5923/j.ijmee.20130202.07.
[11] M.C. Somani, D.A. Porter, L.P. Karjalainen, P.P. Suikkanen, R.D.K. Misra, Process design for tough ductile martensitic steels through direct quenching and partitioning, Mater. Today Proc. 2 (2015) S631–S634, https://doi.org/10.1016/j.matpr.2015.07.363.
[12] O. Haiko, M. Somani, D. Porter, P. Kantanen, J. Kömi, N. Ojala, V. Heino, Comparison of impact-abrasive wear characteristics and performance of direct quenched (DQ) and direct quenched and partitioned (DQ&P) steels, Wear 400–401 (2018) 21–30, https://doi.org/10.1016/j.wear.2017.12.016.
[13] P. Kantanen, M. Somani, A. Kaijalainen, O. Haiko, D. Porter, J. Kömi, Microstructural characterization and mechanical properties of direct quenched and partitioned high-aluminum and high-silicon steels, Metals 9 (2019) 256, https://doi.org/10.3390/met9020256.
[14] C. Garcia-Mateo, T. Sourmail, F.G. Caballero, V. Smanio, M. Kuntz, C. Ziegler, A. Leiro, E. Vuorinen, R. Elvira, T. Teeri, Nanostructured steel industrialisation: plausible reality, Mater. Sci. Technol. 30 (2014) 1071–1078, https://doi.org/10.1179/1743284713Y.0000000428.
[15] B. Liu, W. Li, X. Lu, X. Jia, X. Jin, The effect of retained austenite stability on impact-abrasion wear resistance in carbide-free bainitic steels, Wear 428–429 (2019) 127–136, https://doi.org/10.1016/j.wear.2019.02.032.
[16] P.V. Moghaddam, M. Rinaudo, J. Hardell, E. Vuorinen, B. Prakash, Influence of fracture toughness on two-body abrasive wear of nanostructured carbide-free bainitic steels, Wear 460–461 (2020), 203484, https://doi.org/10.1016/j.wear.2020.203484.
[17] C. Wang, Y. Chang, J. Yang, W. Cao, H. Dong, Y. Wang, Work hardening behavior and stability of retained austenite for quenched and partitioned steels, J. Iron Steel Res. Int. 23 (2016) 130–137, https://doi.org/10.1016/S1006-706X(16)30024-3.
[18] H.L. Yi, P. Chen, H.K.D.H. Bhadeshia, Optimizing the morphology and stability of retained austenite in a δ-TRIP steel, Metall. Mater. Trans. 45 (2014) 3512–3518, https://doi.org/10.1007/s11661-014-2267-4.
[19] E. Vuorinen, V. Heino, N. Ojala, O. Haiko, A. Hedayati, Erosive-abrasive wear behavior of carbide-free bainitic and boron steels compared in simulated field conditions, Proc. IME J. J. Eng. Tribol. 232 (2018) 3–13, https://doi.org/10.1177/1350650117739125.
[20] S.M. Hasan, D. Chakrabarti, S.B. Singh, Dry rolling/sliding wear behaviour of pearlitic rail and newly developed carbide-free bainitic rail steels, Wear 408–409 (2018) 151–159, https://doi.org/10.1016/j.wear.2018.05.006.
[21] S. das Bakshi, Wear of Fine Pearlite, Nanostructured Bainite and Martensite, Doctoral Dissertation, University of Cambridge, 2016.
[22] K. Valtonen, N. Ojala, O. Haiko, V.-T. Kuokkala, Comparison of various high-stress wear conditions and wear performance of martensitic steels, Wear 426–427 (2019) 3–13, https://doi.org/10.1016/j.wear.2018.12.006.
[23] O. Haiko, V. Javaheri, K. Valtonen, A. Kaijalainen, J. Hannula, J. Kömi, Effect of prior austenite grain size on the abrasive wear resistance of ultra-high strength martensitic steels, Wear 454–455 (2020), 203336, https://doi.org/10.1016/j.wear.2020.203336.
[24] V. Javaheri, O. Haiko, S. Sadeghpour, K. Valtonen, J. Kömi, D. Porter, On the role of grain size on slurry erosion behavior of a novel medium-carbon, low-alloy pipeline steel after induction hardening, Wear 476 (2021), 203678, https://doi.org/10.1016/j.wear.2021.203678.
[25] O. Haiko, K. Valtonen, A. Kaijalainen, S. Uusikallio, J. Hannula, T. Liimatainen, J. Kömi, Effect of tempering on the impact-abrasive and abrasive wear resistance of ultra-high strength steels, Wear 440–441 (2019), 203098, https://doi.org/10.1016/j.wear.2019.203098.
[26] N. Ojala, K. Valtonen, V. Heino, M. Kallio, J. Aaltonen, P. Siitonen, V.-T. Kuokkala, Effects of composition and microstructure on the abrasive wear performance of quenched wear resistant steels, Wear 317 (2014) 225–232, https://doi.org/10.1016/j.wear.2014.06.003.
[27] V. Javaheri, S. Sadeghpour, P. Karjalainen, M. Lindroos, O. Haiko, N. Sarmadi, S. Pallaspuro, K. Valtonen, F. Pahlevani, A. Laukkanen, J. Kömi, Formation of nanostructured surface layer, the white layer, through solid particles impingement during slurry erosion in a martensitic medium-carbon steel, Wear 496–497 (2022), 204301, https://doi.org/10.1016/j.wear.2022.204301.
[28] S. Ghosh, P. Kaikkonen, V. Javaheri, A. Kaijalainen, I. Miettunen, M. Somani, J. Kömi, S. Pallaspuro, Design of tough, ductile direct quenched and partitioned advanced high-strength steel with tailored silicon content, J. Mater. Res. Technol. 17 (2022) 1390–1407, https://doi.org/10.1016/j.jmrt.2022.01.073.
[29] P.M. Kaikkonen, M.C. Somani, I.H. Miettunen, D.A. Porter, S.T. Pallaspuro, J. I. Kömi, Constitutive flow behaviour of austenite at low temperatures and its influence on bainite transformation characteristics of ausformed medium-carbon steel, Mater. Sci. Eng., A 775 (2020), 138980, https://doi.org/10.1016/j.msea.2020.138980.
[30] ASTM E562-01, Standard Test Method for Determining Volume Fraction by Systematic Manual Point Count, 2000.
[31] H.M. Rietveld, A profile refinement method for nuclear and magnetic structures, J. Appl. Crystallogr. 2 (1969) 65–71, https://doi.org/10.1107/S0021889869006558.
[32] M. Morawiec, A. Grajcar, Some aspects of the determination of retained austenite using the Rietveld refinement, J. Achiev. Mater. Manuf. Eng. 1 (2017) 11–17, https://doi.org/10.5604/01.3001.0010.1442.
[33] W.W. Sun, Y.X. Wu, S.C. Yang, C.R. Hutchinson, Advanced high strength steel (AHSS) development through chemical patterning of austenite, Scripta Mater. 146 (2018) 60–63, https://doi.org/10.1016/j.scriptamat.2017.11.007.
[34] O. Seppälä, S. Uusikallio, J. Larkiola, A tool for computer-aided calculation of grain size, in: D. Szeliga, L. Rauch (Eds.), Book of Abstracts of the XXVI International Conference on Computer Methods in Materials Technology KomPlasTech 2019, 2019, ISBN 978-83-947091-4-3, pp. 128–130. http://www.aknet.biz.pl/.
[35] M.N. Yoozbashi, S. Yazdani, XRD and TEM study of bainitic ferrite plate thickness in nanostructured, carbide free bainitic steels, Mater. Chem. Phys. 160 (2015) 148–154, https://doi.org/10.1016/j.matchemphys.2015.03.071.
[36] C. Garcia-Mateo, J.A. Jimenez, B. Lopez-Ezquerra, R. Rementeria, L. Morales-Rivas, M. Kuntz, F.G. Caballero, Analyzing the scale of the bainitic ferrite plates by XRD, SEM and TEM, Mater. Char. 122 (2016) 83–89, https://doi.org/10.1016/j.matchar.2016.10.023.
[37] Y.Y. Yang, H.S. Fang, W.G. Huang, A study on wear resistance of the white layer, Tribol. Int. 29 (1996) 425–428, https://doi.org/10.1016/0301-679X(95)00099-P.
[38] A.R. Chintha, Metallurgical aspects of steels designed to resist abrasion, and impact-abrasion wear, Mater. Sci. Technol. 35 (2019) 1133–1148, https://doi.org/10.1080/02670836.2019.1615669.
[39] V. Heino, K. Valtonen, P. Kivikytö-Reponen, P. Siitonen, V.T. Kuokkala, Characterization of the effects of embedded quartz layer on wear rates in abrasive wear, Wear 308 (2013) 174–179, https://doi.org/10.1016/j.wear.2013.06.019.
[40] V. Heino, P. Kivikytö-Reponen, M. Vippola, K. Valtonen, V.-T. Kuokkala, Wear reducing effect of embedded quartz abrasives in crushing-pin-on-disc procedure, Tribol. Online 7 (2012) 179–183, https://doi.org/10.2474/trol.7.179.
[41] Y.-Y. Yang, H.-S. Fang, Y.-K. Zheng, Z.-G. Yang, Z.-L. Jiang, The failure models induced by white layers during impact wear, Wear 185 (1995) 17–22, https://doi.org/10.1016/0043-1648(94)06586-1.
[42] P. Zhang, J.X. Chen, J. Li, H.L. Yu, X.H. Tu, W. Li, Microstructure evolution mechanism of carbides-free bainite steel during impact abrasive wear, Wear 486–487 (2021), 204074, https://doi.org/10.1016/j.wear.2021.204074.
[43] P. Kaikkonen, M.C. Somani, A. Pohjonen, V. Javaheri, J. Kömi, Evaluation of a processing route and microstructural characteristics for the development of ultrafine bainite in low-temperature ausformed medium-carbon steels, J. Mater. Eng. Perform. (2022), https://doi.org/10.1007/s11665-022-07686-4.
[44] B. Liu, W. Li, X. Lu, X. Jia, X. Jin, An integrated model of impact-abrasive wear in bainitic steels containing retained austenite, Wear 440–441 (2019), 203088, https://doi.org/10.1016/j.wear.2019.203088.
[45] M. Koyama, Z. Zhang, M. Wang, D. Ponge, D. Raabe, K. Tsuzaki, H. Noguchi, C. C. Tasan, Bone-like crack resistance in hierarchical metastable nanolaminate steels, Science 355 (2017) 1055–1057, https://doi.org/10.1126/science.aal2766, 1979.
[46] P.V. Moghaddam, J. Hardell, E. Vuorinen, B. Prakash, Effect of retained austenite on adhesion-dominated wear of nanostructured carbide-free bainitic steel, Tribol. Int. 150 (2020), 106348, https://doi.org/10.1016/j.triboint.2020.106348.
[47] S.P. Neog, S. das Bakshi, S. Das, Effect of normal loading on microstructural evolution and sliding wear behaviour of novel continuously cooled carbide free bainitic steel, Tribol. Int. 157 (2021), 106846, https://doi.org/10.1016/j.triboint.2020.106846.